Trace Organic Contaminant Removal from Municipal Wastewater by Styrenic β-Cyclodextrin Polymers

Zhi-Wei Lin, Emma F. Shapiro, Francisco J. Barajas-Rodriguez, Arsen Gaisin, Mohamed Ateia, John Currie, Damian E. Helbling, Rosa Gwinn, Aaron I. Packman, and William R. Dichtel*

Read Online

ACCESS | Metrics & More | Article Recommendations | Supporting Information

ABSTRACT: Trace organic contaminants (TrOCs) present major removal challenges for wastewater treatment. TrOCs, such as perfluoroalkyl and polyfluoroalkyl substances (PFAS), are associated with chronic toxicity at ng L^{-1} exposure levels and should be removed from wastewater to enable safe reuse and release of treated effluents. Established adsorbents, such as granular activated carbon (GAC), exhibit variable TrOC removal and fouling by wastewater constituents. These shortcomings motivate the development of selective novel adsorbents that also maintain robust performance in wastewater. Cross-linked β-cyclodextrin (β-CD) polymers are promising adsorbents with demonstrated TrOC removal efficacy. Here, we report a simplified and potentially scalable synthesis of a porous polymer composed of styrene-linked β-CD and cationic ammonium groups. Batch adsorption experiments demonstrate that the polymer is a selective adsorbent exhibiting complete removal for six out of 13 contaminants with less adsorption inhibition than GAC in wastewater. The polymer also exhibits faster adsorption kinetics than GAC and ion exchange (IX) resin, higher adsorption affinity for PFAS than GAC, and is regenerable by solvent wash. Rapid small-scale column tests show that the polymer exhibits later breakthrough times compared to GAC and IX resin. These results demonstrate the potential for β-CD polymers to remediate TrOCs from complex water matrices.

KEYWORDS: PFAS, cyclodextrin polymer, wastewater, adsorption, RSSCT, organic contaminants
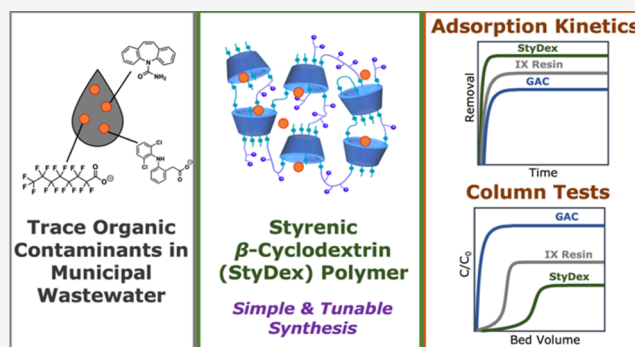
INTRODUCTION

Demand for safe and reliable freshwater resources will intensify in the near future due to population increase, climate change, and water pollution. Wastewater reclamation, particularly from municipal sources, can reduce freshwater demands[1,2] and provide recoverable sources of nutrients, as well as other environmental benefits associated with cleaner water.[3,4] Using reclaimed wastewater for nonpotable purposes, such as public landscape irrigation and industrial cooling, has been widely adopted by municipalities in various countries, particularly in regions impacted by water scarcity.[5−7] However, potable reuse and irrigation of agriculture, which accounts for 80% of the global freshwater consumption,[8] face challenges associated with the removal of trace organic contaminants (TrOCs).[9,10] Some contaminants,[11] which include pharmaceuticals and personal care products,[12] industrial chemicals,[13] and per- and polyfluoroalkyl substances (PFAS),[14,15] are associated with chronic toxicity.[16,17] However, much is unknown about the negative effects of exposure to complex mixtures of TrOCs. Despite these challenges, conventional and advanced wastewater treatment methods are often insufficient in removing or degrading all TrOCs,[18,19] making wastewater treatment plants (WWTPs) a significant anthropogenic source of TrOCs in

local lakes, rivers, and reservoirs, where contaminants are often detected at concentrations ranging from ng L^{-1} to mg L^{-1}.[20]

Adsorption is one of the most economical, effective, and practical approaches for removing organic and inorganic constituents from contaminated water.[19,21] Cross-linked β-cyclodextrin (β-CD) polymers have emerged as promising adsorbents for the removal of PFAS,[22,23] organic dyes,[24,25] and pharmaceuticals[26,27] from water.[28,29] β-CDs are commercially available oligosaccharides that are produced from cornstarch and are found in many commercial products.[30] Their hydrophobic cavity can form stable, size-selective host−guest complexes with many small organic molecules, including some PFAS.[31] We developed several β-CD polymers derived from nucleophilic aromatic substitution reactions between unmodified β-CD and electron-deficient aromatic cross-linkers.[26,32−35] Compared to conventional adsorbents such as granular
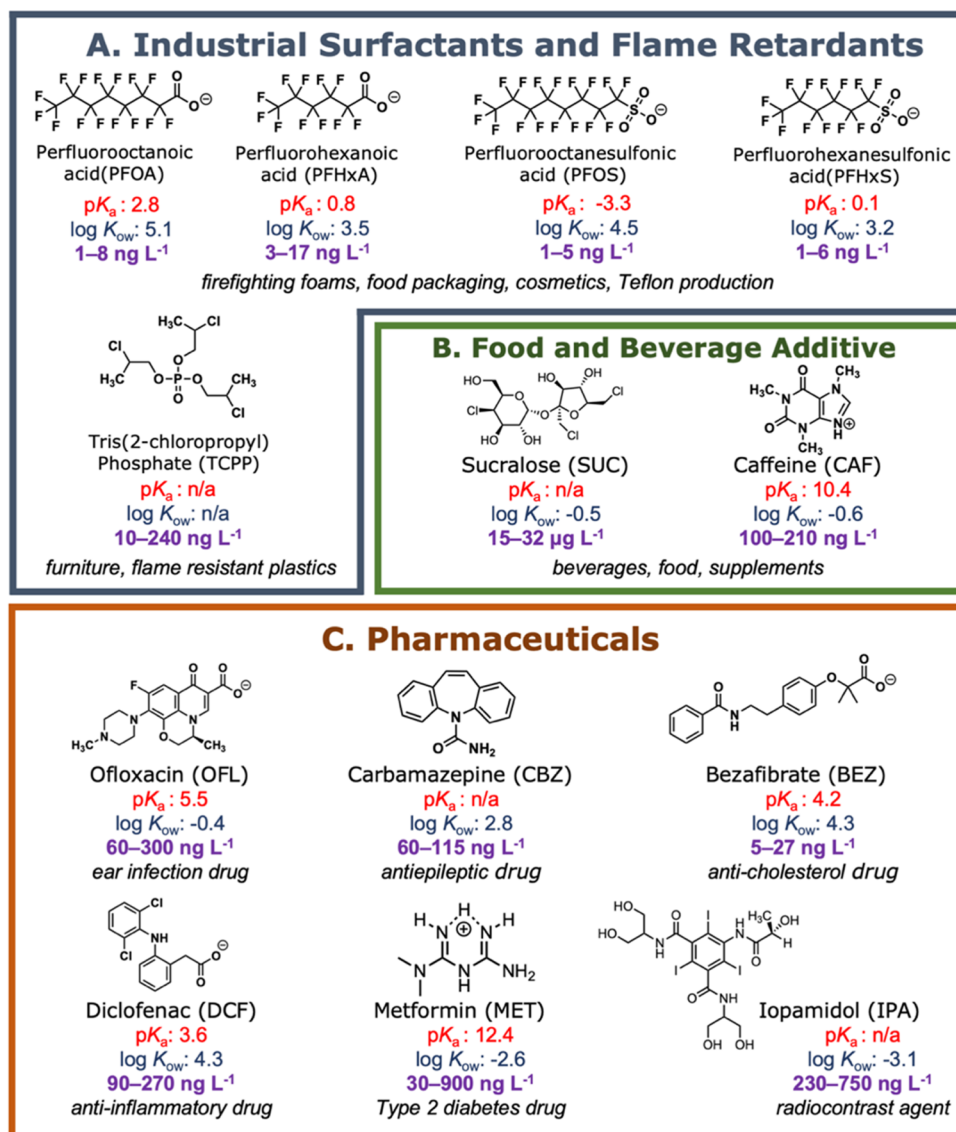
Figure 1. TrOCs in this study fall under three general classes: (A) industrial surfactants and flame retardants, (B) food and beverage additives that are also common indicators of anthropogenic pollution, and (C) common pharmaceuticals. The contaminants are depicted in their protonated and deprotonated states under neutral pH, along with their pK_a and log K_{ow} values.[15,29,30] TrOC background concentrations in different wastewater samples prior to spike addition are reported in purple text as a range in either ng L^{-1} or μg L^{-1}. n/a = not available.

activated carbon (GAC) and ion exchange (IX) resins, these β-CD polymers generally exhibit higher adsorption affinities and faster adsorption kinetics for organic contaminants[26,32−34] and are more resistant to fouling by dissolved organic matter (DOM) and inorganic constituents.[36−38] Despite their promising performance, β-CD polymers based on substitution reactions are limited in their ability to be rationally improved or further modified. We recently reported a new approach to synthesize porous β-CD-containing polymers with tailorable chemical composition, based on copolymerization of a styrene-functionalized β-cyclodextrin (StyDex) derivative with commercially available styrenic and methacrylic comonomers.[23] Based on studies in nanopure water and aqueous electrolyte solutions, the adsorption mechanisms of StyDex are hypothesized to include (1) hydrophobic interactions with the polymer surface; (2) host−guest interactions with the β-CD cavities; and (3) electrostatic attraction with charged comonomers, such as methacrylate derivatives bearing a quaternary ammonium ion. StyDex polymers showed efficient PFAS

removal in nanopure water at a low adsorbent loading of 1 mg L^{-1}. Although many polymer-based adsorbents have demonstrated effective TrOC removal in nanopure water, many adsorbents, including StyDex polymers, have not yet been evaluated under environmentally relevant conditions and within the flow-through systems needed for large-scale engineering implementation.[39]

Here, we report a simplified synthesis of StyDex polymers and evaluated their ability to remove TrOCs from municipal wastewater collected from a WWTP in Illinois, U.S.A. We chose to focus on PFAS, food and beverage additives, and pharmaceuticals that are commonly found in municipal wastewater (Figure 1).[12,14] A StyDex polymer bearing quaternary ammonium groups was synthesized through free radical polymerization. The polymer was evaluated for the removal efficiencies of 13 TrOCs that were spiked into nanopure water and municipal wastewater. Performance was benchmarked to two commercial adsorbents: a regenerable GAC Filtrasorb 600[40] and a single-use IX resin Amberlite

PSR2+.[41] Batch adsorption and rapid small-scale column test (RSSCT) experiments offered important insights into the performance of StyDex polymers for TrOC removal in a complex wastewater matrix. In general, StyDex polymers exhibited superior TrOC removal performance and less removal inhibition by wastewater constituents compared to a representative GAC, and they had similar performance compared with IX resin. StyDex polymers are regenerable and, when packed in fixed-bed columns, demonstrate longer breakthrough times and steeper breakthrough curves, indicating high adsorbent capacities, rapid adsorption kinetics, and narrow mass transfer zones. Together, these studies demonstrate StyDex polymers as promising adsorbents for wastewater reclamation.

■ MATERIALS AND METHODS

Materials. β-Cyclodextrin (97%) was provided by Wacker Chemical and dried at 80 °C under a high vacuum prior to monomer synthesis. Sodium hydroxide, sodium chloride, 2,2′-azobis(2-methylpropionitrile) (AIBN, 98%), 4-vinylbenzyl chloride (90%), and [2-(methacryloyloxy)ethyl] trimethylammonium chloride solution (MATMA, 75% in H_2O) were purchased from Sigma-Aldrich and used as received. A list of 13 TrOCs and their suppliers is provided in Table S1, along with their preparation and storage information. These TrOCs were selected because of their significant environmental concerns and widespread occurrences in municipal wastewater. For batch adsorption experiments, the following consumables: Chromafil Xtra cellulose acetate syringe filter (13 mm, 0.2 μm, Macherey-Nagel), glass LC vials (2 mL, Agilent), cellulose acetate membrane filter (47 mm, 0.2 μm, Sterlitech), Falcon conical centrifuge tubes (15 and 50 mL, Fisher Scientific), and Air-Tite plastic syringes (10 mL, Fisher Scientific) were investigated for nonspecific interactions with the target TrOCs through spike-recovery tests (see Section G in the Supporting Information). For RSSCT experiments, HDPE carboys (5 gal) were purchased from McMaster Carr. Polyether sulfonate (PES) in-line capsule filter (1 μm) was purchased from Waterra. ReaXus M1 Class pumps were purchased from (Teledyne ISCO). PEEK tubing (1/8 and 1/16 in. diameter) was purchased from ChromTech. For LC−MS/MS, Agilent Poroshell 120 guard column (2.11 mm, 2.7 μm) and Agilent Poroshell 120 EC-C18 column (2.1 × 100 mm, 2.7 μm) were purchased from Neta Scientific. Regenerable GAC Filtrasorb 600 was purchased from Calgon Carbon and single-use IX resin Amberlite PSR2+ was provided by DuPont Water Solutions. To enable a direct comparison with StyDex polymers, F600 and PSR2+ were ground and sieved to a 90−125 μm particle diameter to match the size of the StyDex polymers.

Synthesis and Characterization of StyDex Adsorbents. For StyDex monomer synthesis, dry β-CD (10.0 g, 8.81 mmol) and finely ground sodium hydroxide powders (2.50 g, 61.7 mmol) were dissolved in dimethyl sulfoxide (DMSO) (100 mL) and stirred for 30 min. 4-Vinylbenzyl chloride (17.4 mL, 61.7 mmol) was added to the solution, and the mixture was stirred at room temperature for 20 h. The solution was then precipitated into a saturated solution of sodium chloride (1 L) and stirred for 10 min before vacuum filtration. The filtrate was washed with copious amounts of water and dried under high vacuum at room temperature for 20 h to give off-white powders (isolated yield: 94%). The powders were stored at −8 °C and protected from light. Notably, this one-step

StyDex monomer synthesis was simplified from a three-step synthesis described in a previous report.[23]

For free radical polymerization, StyDex monomers (5.00 g) and AIBN (160 mg, 0.974 mmol) were dissolved in DMF (17.0 mL). Two molar equivalents of MATMA (1.31 mL, 5.21 mmol) per mole of StyDex monomer were added as a liquid. The monomer solution was transferred to a dry Schlenk flask, subjected to three freeze−pump−thaw cycles, and heated to 80 °C under continuous N_2 flow. The polymer gelled after 15 min and was heated for an additional 45 min. After 1 h total reaction time, the solid gel was broken apart with a metal spatula, immediately transferred to a standard teabag, and sealed with staples. This teabag was subjected to a Soxhlet extractor with methanol for 15 h before activating the polymer with supercritical CO_2 for 80 washing cycles (isolated yield: 95%). The polymer was ground and sieved into a fine powder between 90 and 125 μm as this size range produces consistent stock adsorbent suspension for batch adsorption experiments. The polymer powder was stored at room temperature and was bench-stable for over a year without a decreased removal performance.

The StyDex monomer was characterized by ^1H and ^{13}C nuclear magnetic resonance (NMR) spectroscopy, matrix-assisted laser desorption/ionization time-of-flight mass spectrometry (MALDI-TOF MS), and Fourier transform infrared (FTIR) spectroscopy. The polymer was characterized by using solid-state cross-polarization magic angle spinning (CPMAS) ^{13}C NMR spectroscopy, N_2 porosimetry, FTIR spectroscopy, and ζ potential. Instrumentation parameters are provided in Section B in the Supporting Information.

Water Samples. Six batches of municipal wastewater effluent were collected at different times between March and October 2022 from the same WWTP in Illinois, U.S.A. during this study. All effluent samples collected received primary and secondary treatment at the plant, but not tertiary disinfection treatment (see Section C in the Supporting Information). Three wastewater samples (WW1−WW3) were used for batch adsorption experiments, and three wastewater samples (WW4−WW6) were used for RSSCT experiments (Table S2). For RSSCT experiments, WW4−WW6 were separately shipped from the WWTP to AECOM's Process Technology Laboratory in Austin, TX. Each batch of wastewater (WW4−WW6) was shipped in three individual carboys (5 gal), which were combined into a larger HDPE drum (20 or 30 gal) to homogenize the contents and reduce variability. Combined wastewater was prefiltered with a PES in-line capsule filter (1 μm) to remove suspended solids and transferred back into three new carboys (5 gal). Each carboy was spiked with TrOCs and used in flow-through columns (RSSCTs). Methanol, which is the solvent for contaminant cocktails, constitutes 0.2 vol % in each carboy (Table S2). For batch adsorption experiments, WW1−WW3 were not homogenized and were used as collected without any modification or additives other than the TrOC spike. Each TrOC-spiked batch adsorption sample also contains 0.2 vol % methanol. Wastewater samples were characterized for pH, dissolved oxygen (DO), dissolved organic carbon (DOC), total suspended solids (TSS), total dissolved solids (TDS), chemical oxygen demand (COD), Red-Ox potential, and inorganic ion concentrations using standard analytical methods (Table S2).

Batch Adsorption Experiments. The consumables used in batch adsorption experiments were tested for nonspecific interactions with the target TrOCs through spike-recovery

tests (see Section G in the Supporting Information). Falcon centrifuge tubes (15 or 50 mL) were filled with either 14 or 48 mL of nanopure water or wastewater. TrOCs were initially spiked at 500 ng L^{-1} in nanopure water or wastewater for equilibrium adsorption and adsorption kinetics experiments and ranged from 100 to 8000 ng L^{-1} for adsorption isotherm experiments. Actual TrOC concentrations in experiments with wastewater will vary based on background concentrations already present in the collected samples (Figure 1). To prepare an adsorbent loading of 100 mg L^{-1}, a stock adsorbent suspension was first created. For example, 20 mg of adsorbent (sieved to 90−125 μm) was added to 20 mL of nanopure water to create a 1 g L^{-1} suspension. The suspension was mixed with a vortex mixer for 1 min, sonicated for 1 min to break apart aggregates, and then stirred for 30 min at 300 rpm. To each Falcon tube, appropriate volumes of water samples, contaminant cocktails (13 TrOCs, each at 1 mg L^{-1}), and the adsorbent suspension (1 g L^{-1}) were added successively to reach their testing concentrations. Sample tubes were placed in a Thermo Scientific Solaris 2000 orbital shaker at 200 rpm at room temperature for 24 h for equilibrium adsorption and adsorption isotherm experiments and 5 min to 24 h for adsorption kinetics experiments. Following the specified contact time, samples were filtered through a 0.2 μm cellulose acetate syringe filter (Chromafil Xtra) and collected in 6 mL volumes. Spike controls (no adsorbents) and negative controls (no adsorbents or spiked TrOC) were prepared for each experiment. All experiments were performed in triplicate. Regeneration experiments are described in Section H in the Supporting Information.

Design of RSSCT Experiments. Design parameters were calculated to simulate a large-scale column containing a granular adsorbent with an average particle diameter of 1000 μm under the assumptions of constant diffusivity (CD) and proportional diffusivity (PD) models that were developed to evaluate activated carbon.[42] A simulated large-scale empty-bed contact time (EBCT) of 10 min was selected based on industry standards used for TrOC adsorption. Scaling of the EBCT for an RSSCT experiment is obtained by eq 1:

$$\frac{\text{EBCT}_{\text{SC}}}{\text{EBCT}_{\text{LC}}} = \left(\frac{d_{\text{p,SC}}}{d_{\text{p,LC}}}\right)^{2-X} \tag{1}$$

in which EBCT$_{\text{SC}}$ and EBCT$_{\text{LC}}$ are the EBCTs of the small and large columns, respectively; $d_{\text{p,SC}}$ and $d_{\text{p,LC}}$ are the particle diameters of the adsorbent for the small and large columns, respectively; and X defines the dependence of the intraparticle diffusion coefficient on particle size. For a CD approach, $X = 0$. For a PD approach, $X = 0.5$. The desired target small-scale particle diameter was defined as 50 times smaller than the RSSCT column diameter to avoid channeling (ASTM D6586-03). The flow regime for the RSSCTs was selected to meet a Reynolds number between 0.3 and 0.4, as suggested by the ASTM methodology. Once the flow rate and the EBCT were established, the RSSCT adsorbent bed volume (BV) and depths were calculated. The resulting design parameters for the RSSCT experiments are provided in Table S3.

The materials (e.g., glass wool, PEEK tubing) used in RSSCT experiments were also tested for nonspecific interactions with the target TrOCs (see Section G in the Supporting Information). For each RSSCT experiment, homogenized and prefiltered wastewater was spiked with an estimated concentration of 500 ng L^{-1} per contaminant and

pumped (ReaXus M1 Class Pumps, Teledyne ISCO) through the packed column with a fixed hydraulic loading rate (HLR) between 0.20 and 0.25 cm s^{-1}, based on a laminar Reynolds number to minimize issues with pressure loss across the column. To pack the column, Cationic StyDex, F600, or PSR2+ (sieved to 90−125 μm) was mixed with nanopure water to create a slurry with a 1:1 water-to-adsorbent ratio. The slurry was packed into a stainless-steel chromatography column (Restek) with a 0.46 cm internal diameter to achieve a predetermined depth. Glass wool was used to fill the void space above and below adsorbent. Prior to each RSSCT experiment, flow rates were monitored for at least 4 h to ensure stability of the pump, and then 50,000 bed volumes (BV) of TrOC solution were pumped through the column. Effluent samples were taken daily in 50 mL HDPE bottles and stored under refrigeration until analysis. Influent samples were collected daily from the carboy to monitor any losses and account for changes in TrOC concentration.

TrOC Quantification. The quantification of TrOCs in samples from batch adsorption and RSSCT experiments was performed by means of ultrahigh-performance liquid chromatography (UPLC) coupled with a SCIEX QTRAP 6500+ triple quadrupole and linear ion trap mass spectrometer (MS). Prior to each analysis, samples were filtered through a 0.2 μm cellulose acetate syringe filter (Chromafil Xtra). Analytes were first separated on an Agilent Poroshell 120 EC-C18 column (2.1 × 100 mm, 2.7 μm) fitted with a Poroshell 120 guard column (2.11 mm, 2.7 μm), using LCMS-grade water, methanol, and acetonitrile as eluents. Analytical information for all TrOCs is provided in Table S4. The column temperature was held constant at 40 °C. UPLC-MS was operated with electrospray ionization in positive and negative polarity mode. Calibration standards (n = 10) were prepared in duplicate in nanopure water with concentrations between 0 and 1000 ng L^{-1} for all experiments, except adsorption isotherm experiments, for which calibration standards had a low range of 0−1000 ng L^{-1} and a high range of 1000−10,000 ng L^{-1}. Calibration standards were prepared for each analysis instead of using isotopically labeled internal standards. Additional analytical information is provided in Section E in the Supporting Information.

Data Analysis. The removal efficiency of each TrOC in each sample was calculated as

$$R = \frac{C_0 - C_t}{C_0} \times 100 \tag{2}$$

in which R is the percent removal of each TrOC; C_0 (ng L^{-1}) is the average measured concentration of a TrOC in spike control (no adsorbent), which also includes background concentration of the TrOC in wastewater samples; and C_t (ng L^{-1}) is the concentration of each TrOC in water at sampling time t. Any incidental TrOC losses were assumed to occur to the same extent in control and experimental samples and were not explicitly considered in eq 2. The adsorption density at sampling time t was calculated as

$$q_t = \frac{C_0 - C_t}{C_{\text{ads}}} \tag{3}$$

in which q_t (μg g^{-1}) is the adsorption density; C_0 (ng L^{-1}) is the average measured concentration of a TrOC in spike controls; C_t (ng L^{-1}) is the concentration of each TrOC in water at sampling time t; and C_{ads} is the concentration of the

adsorbent. To obtain a quantitative metric to compare adsorbent kinetics for each TrOC, Ho and McKay's pseudo-second-order adsorption model[43] was applied using nonlinear least-squares regression of eq 4

$$\frac{t}{q_t} = \frac{t}{q_e} + \frac{1}{k_{obs}q_e^2} \tag{4}$$

in which q_t (μg g^{-1}) is the adsorption density calculated using eq 3; q_e (μg g^{-1}) is the equilibrium adsorption density; and k_{obs} (g μg^{-1} h^{-1}) is the adsorption rate constant. Adsorption density (q_t) measurements that resulted in a negative value (7 cases for all TrOC-adsorbent pairs across all triplicate samples) were omitted from the estimation of k_{obs}. The distribution coefficient K_D (L μg^{-1}) was calculated from the slope of the linear region of the adsorption isotherm data for each adsorbent−TrOC pair and is interpreted as

$$K_D = \frac{q_e}{C_e} \tag{5}$$

in which q_e (μg g^{-1}) is the equilibrium adsorption density and C_e (μg L^{-1}) is the equilibrium concentration of each TrOC. Adsorption isotherm data were also fitted to Langmuir and Freundlich adsorption models using nonlinear least-squares regression of eqs 6 and 7, respectively,

$$q_e = \frac{q_{max}K_L C_e}{1 + K_L C_e} \tag{6}$$

in which q_e (μg g^{-1}) is the equilibrium adsorption density; C_e (μg L^{-1}) is the equilibrium concentration of each TrOC; q_{max} (μg g^{-1}) is the adsorption capacity; and K_L (L μg^{-1}) is the Langmuir constant for adsorption affinity.

$$q_e = K_F C_e^{1/n} \tag{7}$$

in which q_e (μg g^{-1}) is the equilibrium adsorption density; C_e (μg L^{-1}) is the equilibrium concentration of each TrOC; n is an indicator of the intensity of adsorption; and K_F (μg g^{-1}) (L μg^{-1})$^{1/n}$ is the Freundlich constant.

■ RESULTS AND DISCUSSION

Synthesis and Characterization of StyDex Monomer and Polymer. To prepare StyDex monomers, styrene groups were installed at the hydroxyl groups at the 2′, 3′, and 6′ positions of β-CD via direct etherification reactions with 4-vinylbenzyl chloride as the electrophile (Scheme 1A). This reaction was performed at room temperature with an isolated yield of 94%, after precipitation and washing of the solid product. The ^{1}H NMR spectrum of StyDex monomer indicated successful installation of styrene groups, based on the appearance of aromatic and vinyl proton resonances in the 5.0−7.5 ppm region (Figure S1). On average, 7.6 styrene groups per β-CD molecule were installed, as determined by the integration of aromatic proton resonances relative to β-CD proton resonances in the 3.5−5.0 ppm region (see Section F in the Supporting Information). Despite the primary hydroxyl groups (6′) being less sterically hindered and more nucleophilic than the secondary hydroxyl groups (2′ and 3′), the etherification in the presence of NaOH and 4-vinylbenzyl chloride was not selective, yielding StyDex monomers with a distribution of styrene groups at each of these positions. Based on the broadening of the β-CD proton resonances, we assign the styrene-functionalized monomer to have polymerizable

Scheme 1. Synthesis of Styrene-Functionalized Cyclodextrin (StyDex) Monomer and Polymer
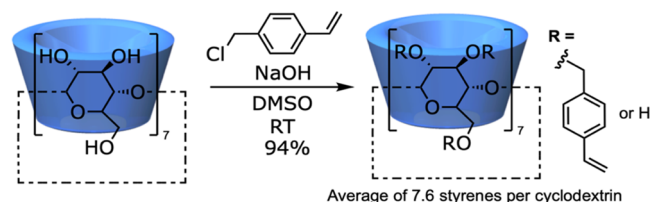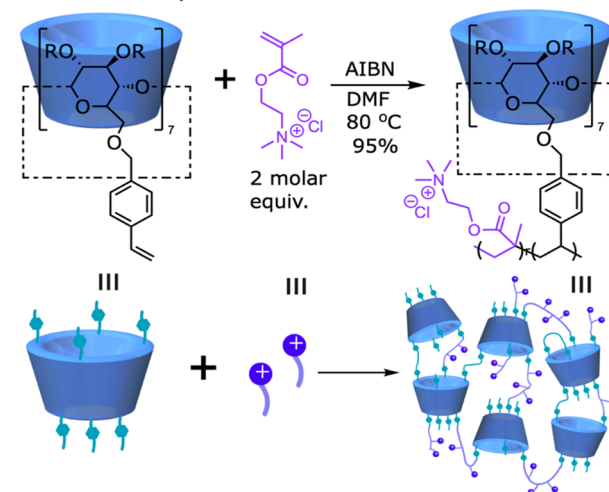
styrene groups on both faces of the β-CD ring. In contrast, we previously prepared a StyDex monomer that was functionalized only at the 6′ position, and its NMR spectrum showed much more well-defined resonances.[23] MALDI-TOF MS of StyDex monomer was also consistent with the incorporation of 7.6 average styrene groups per β-CD molecule, based on a distribution of [M + Na]$^+$ adducts ranging from 1388.46 to 2549.59 m/z in the full-scan chromatogram (Figure S2). The most abundant peaks, 1969.53 and 2085.54 m/z, correspond to the theoretical masses of seven and eight styrene groups per β-CD molecule, respectively. FTIR spectroscopy was also consistent with the expected structure (Figure S3).

The styrene groups of StyDex monomers are potentially compatible with hundreds of commercially available vinyl comonomers and different radical polymerization methods. This versatility is advantageous in developing and tailoring numerous polymer compositions to target a broad scope of TrOCs. For this study, we prepared a polymer based on the StyDex monomer and MATA, a cationic methacrylate monomer bearing quaternary ammonium groups, which were copolymerized using AIBN in DMF at 80 °C, with an isolated yield of 95% following Soxhlet extraction in methanol and activation by supercritical CO_2 washing (Scheme 1B). Cationic StyDex formed as a porous and cross-linked polymer network with a permanent surface charge. Solid-state CPMAS ^{13}C NMR spectroscopy confirmed the successful incorporation of the comonomers (Figure S4). The resonance corresponding to the vinyl carbons (113 ppm) of the StyDex monomer was not detected, indicating a high degree of cross-linking of the styrene groups. The resonances corresponding to the polymer backbone were detected in the broadened alkane regions (20−55 ppm). Carbonyl carbons of the comonomers were detected at around 180 ppm. Furthermore, the characteristic N-methyl

carbons (55 ppm) were detected in the spectrum of Cationic StyDex. The porosity and Brunauer−Emmett−Teller surface area (S_{BET}) of Cationic StyDex, F600, and PSR2+ were characterized by N_2 porosimetry (Table 1). Cationic StyDex

Table 1. Characterization of the Adsorbents

adsorbent	comonomer charge	ζ-potential (mV)[a]	BET surface area (m^2 g^{-1})	isolated yield (%)
Cationic StyDex	cationic	14.1 ± 0.7	250	95
F600	n/a	−29.2 ± 1.1	810	n/a
PSR2+	cationic	12.8 ± 2.3	nonporous	n/a

[a]ζ potentials were measured in 10 mM NaCl (pH = 7) at room temperature; n/a: not applicable.

exhibited a permanent porosity and S_{BET} of 250 m^2 g^{-1} (Figure S4), whereas F600 exhibited an S_{BET} of 810 m^2 g^{-1} (Figure S5). PSR2+ was not porous under these conditions (Figure S6). Cationic StyDex and PSR2+ were found to have strongly positive surface charges, corresponding to ζ potentials of 14.1 ± 0.7 and 12.8 ± 2.3 mV, respectively (Table 1). This is consistent with the incorporation of free cations into the polymer and resin. F600 was found to have a strongly negative surface charge, corresponding to a ζ potential of −29.2 ± 1.1 mV. The FTIR spectrum of Cationic StyDex (Figure S7) was consistent with its expected structures. These measurements confirmed the porous and cross-linked nature of Cationic StyDex.

Characterization of Wastewater Effluents. Six wastewater effluent samples (WW1−WW6) contained various background concentrations of TrOCs (Figure 1). Based on multiple analyses of the effluent samples, PFOA (1−8 ng L^{-1}), PFOS (1−5 ng L^{-1}), PFHxA (3−17 ng L^{-1}), and PFHxS (1−6 ng L^{-1}) levels detected are similar to the typical concentrations reported in many drinking water and wastewater samples,[44,45] which are on par with the recent U.S. EPA proposed enforceable maximum contaminant levels (MCLs) for drinking water (e.g., 4 ng L^{-1} for PFOS and PFOA). To our knowledge, DCF (90−270 ng L^{-1}), SUC (15−32 μg L^{-1}), CAF (100−210 μg L^{-1}), BEZ (5−27 ng L^{-1}), and the rest of the TrOCs are within the expected range reported by other WWTPs in the United States.[46,47]

The wastewater samples were also characterized for general water quality parameters, including pH, DO, DOC, TDS, TSS, COD, and inorganic ion concentrations (Table S2). The pH values of WW1−WW6 (7.3−7.7) were slightly higher than the pH measurements (7.0−7.4) reported by the WWTP for post disinfected effluent. All TrOC-spiked samples contained 0.2 vol % of methanol. The addition of methanol resulted in an increase in DOC levels, such as 394 mg L^{-1} for WW5 (Table S2). However, considering each TrOC-spiked sample contained a low levels of methanol, we suspect methanol exerts a negligible effect on adsorption. The COD and TDS levels in WW4−WW6 used in RSSCT experiments were abnormally higher than the typical levels expected, such as 2017 and 429 mg L^{-1}, respectively, for WW4. We attribute these abnormal levels to the wastewater being kept at room temperature during the shipment process and for the duration of the RSSCT experiments, which enabled substantial autotrophic bacterial growth. This growth is further promoted by the addition of methanol. WW1−WW3 were stored at 4 °C for the duration of the batch adsorption experiments.

Equilibrium Adsorption of TrOCs. We first evaluated the equilibrium removal efficiencies of 100 mg L^{-1} Cationic StyDex, F600, and PSR2+ for 13 TrOCs initially spiked at 500 ng L^{-1} in nanopure water and three different batches of wastewater with a 24 h contact time, which is sufficient to reach equilibrium removal, based on similar removal efficiencies observed in wastewater samples with a 48 h contact time (Figure S13). In past studies, we typically evaluated 10 mg L^{-1} adsorbents, and even as low as 1 mg L^{-1} in nanopure water and engineered water systems.[23] Removal was observed with a similar trend at 10 mg L^{-1} loading for all three adsorbents, but to an overall reduced efficiency (Figure S14).

In nanopure water, Cationic StyDex achieved nearly complete removal of PFOA, PFOS, PFHxA, PFHxS, BEZ, and DCF (Figure 2A). We attribute the effective removal of
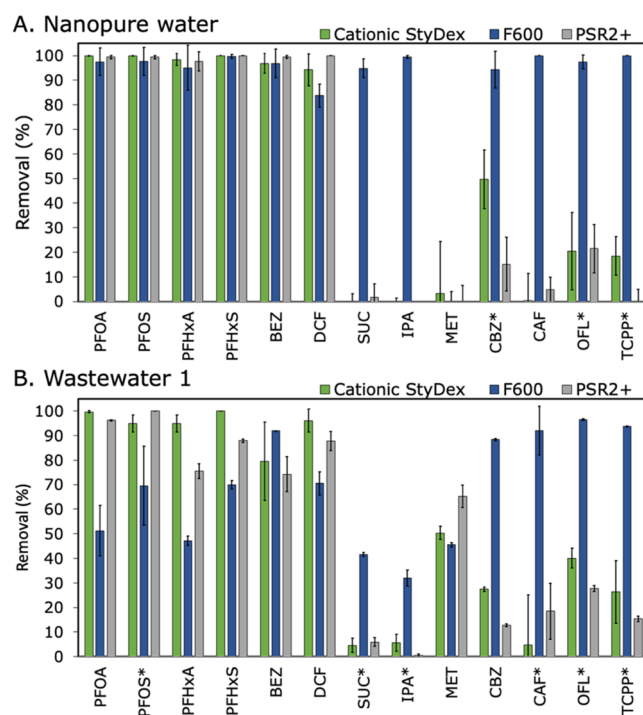

Figure 2. Equilibrium adsorption of TrOCs by Cationic StyDex (green bar), F600 (blue bar), and PSR2+ (gray bar) in (A) nanopure water and (B) WW1 with a contact time of 24 h at room temperature. TrOCs were initially spiked at a concentration of 500 ng L^{-1}. Adsorbents were loaded at 100 mg L^{-1}. Three experiments were performed in WW1 and WW3 and plotted separately. The removal results in WW2 and WW3 are provided in Figure S15. Asterisk (*) denotes TrOC matrix recovery outside of the acceptable range of ±20%. Error bars represent the standard deviation of six replicates in nanopure water and three replicates in wastewater.

Cationic StyDex to its cationic ammonium groups that electrostatically attract anionic TrOCs, as well as polymer surfaces and β-CD cavities that form hydrophobic interactions with TrOCs. However, Cationic StyDex exhibited little to no removal for the other seven TrOCs, which may be attributed to steric hindrance due to the large molecular size of some TrOCs, such as SUC and IPA. This observation was consistent with our prior study that established quantitative structure−activity relationships between several physicochemical properties (e.g., molecular size and charge) of a diverse set of TrOCs and their measured adsorption affinity by a porous β-CD
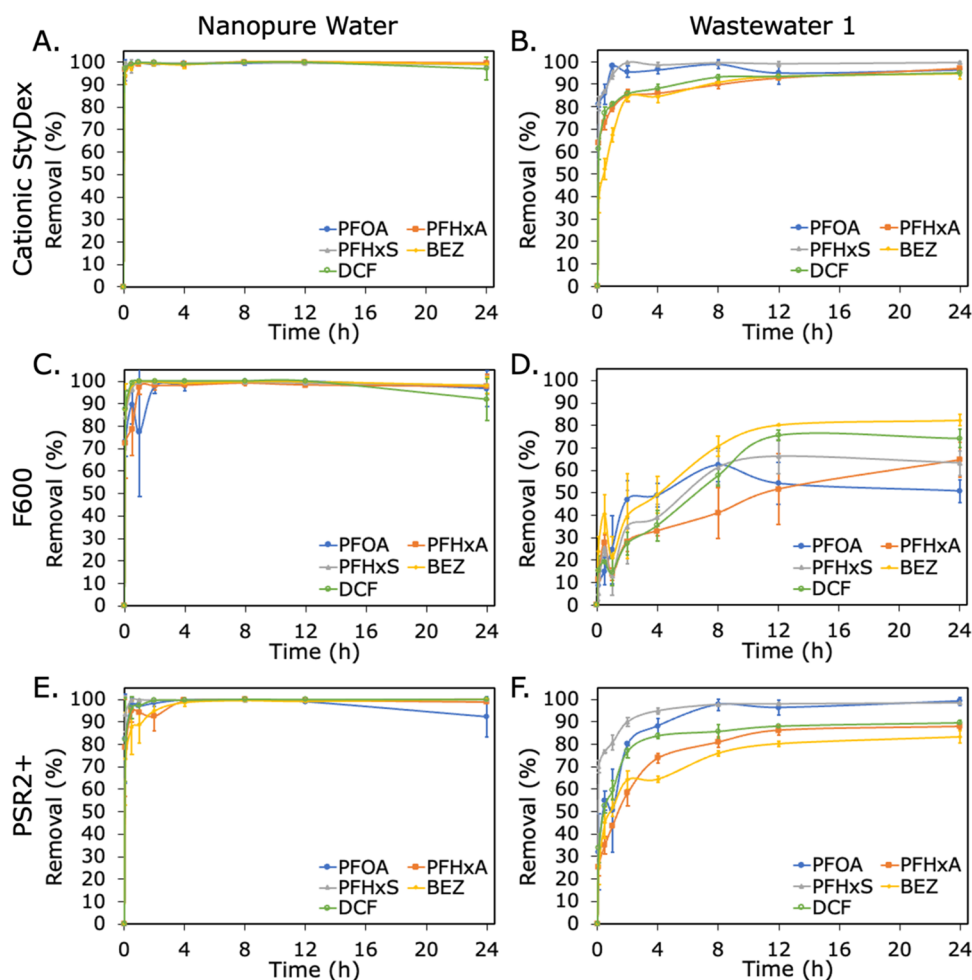
Figure 3. Adsorption kinetics of TrOCs by Cationic StyDex (A, B), F600 (C, D), and PSR2+ (E, F) in nanopure water (left) and WW1 (right) with contact times of 5 min to 24 h at room temperature. TrOCs were initially spiked at 500 ng L^{-1}. Adsorbents were loaded at 100 mg L^{-1}. Two experiments were performed in WW1 and WW2 and plotted separately. Additional kinetics result in WW2 is provided in Figure S19. Error bars represent the standard deviation of six replicates in nanopure water and three replicates in wastewater.

polymer based on the previous generation of cross-linking chemistry.[38] In particular, we attributed the poor adsorption affinities of the previous generation of materials for SUC, TCPP, and IPA to their relatively large molecular sizes. We also observed a trend between log K_{ow} of the TrOC and its removal efficiency by Cationic StyDex, particularly SUC (log K_{ow}: −0.5), IPA (log K_{ow}: −3.1), MET (log K_{ow}: −2.6), CAF (log K_{ow}: −0.6) and OFL (log K_{ow}: −0.4) were inefficiently removed compared to the selected PFAS (log K_{ow}: 3.2−5.1), BEZ (log K_{ow}: 4.3), and DCF (log K_{ow}: 4.3) (Figure 1). This trend suggests that the studied formulation of the Cationic StyDex polymer does not efficiently remove the relatively hydrophilic TrOCs. Interestingly, CBZ has a log K_{ow} of 2.8, suggesting that it can also be effectively removed through hydrophobic interactions, but its removal efficiency was only 50 ± 11% in nanopure water, which suggests that other factors also influence adsorption (Figure 2A). PSR2+ exhibited a removal profile similar to that of Cationic StyDex in nanopure water, with near-complete removal of the selected PFAS, BEZ, and DCF. In contrast, F600 demonstrated effective equilibrium removal for all TrOCs except MET in nanopure water. We observed near-complete removal of PFHxA and PFHxS by F600, despite the fact that GACs generally have poor affinities for shorter-chain PFAS. This

result may be explained by the high adsorbent loading of 100 mg L^{-1} and low initial PFAS concentration of 500 ng L^{-1} in nanopure water. Although F600, PSR2+, and Cationic StyDex achieved similar extents of removal of the selected PFAS, BEZ, and DCF in nanopure water, the adsorbents performed differently in wastewater.

Conventional adsorbents are susceptible to fouling by DOM and inorganic constituents and competitive adsorption among TrOCs in complex water matrices, which significantly limit their wider implementation.[37] Cationic StyDex, F600, and PSR2+ exhibited different degrees of reduced adsorption performance, which we observed in separate experiments performed with three different batches of wastewater (Figures 2B and S15). Among the three adsorbents, F600 experienced the greatest inhibition in adsorption performance in WW1−WW3, such as 47% PFHxA removal in WW1 relative to 98% in nanopure water or 70% DCF removal relative to 96% (Figure 2B). The removal of SUC decreased from 92% in nanopure water to 41% in WW1 most likely due to significantly higher background SUC concentration (15−32 μg L^{-1}) that saturated F600. Similar levels of removal inhibition were also observed for F600 in WW2 and WW3 (Figure S15) despite batch-to-batch variation in the wastewater composition (Table S2). F600 removal results were generally consistent in different

wastewaters (Table S6), with coefficient of variation (CV) < 20% for most TrOC results collected from WW1−WW3 except MET (68%), PFOS (29%), and IPA (39%). In contrast, PSR2+ experienced some removal inhibition in WW1−WW3, such as 74 and 84% PFHxA removal in WW1 and WW3, respectively, relative to 99% removal in nanopure water (Figures 2B and S15B). PSR2+ results were somewhat consistent in different wastewater, with CV < 20% for most TrOC except SUC (97%), MET (129%), OFL (96%), IPA (143%), CAF (170%), and CBZ (23%) (Table S6).

Cationic StyDex experienced minimal removal inhibition and exhibited nearly complete removal of the selected PFAS, BEZ, and DCF in WW1−WW3, which are consistent with past studies that demonstrated β-CD polymers retain robust performance even in complex matrices with high concentrations of DOM and inorganic constituents.[36,37] Additionally, the adsorption competition from nontarget contaminants and a myriad of inorganic constituents that are present in wastewater further demonstrate the selectivity of Cationic StyDex toward the target TrOCs, particularly PFAS. Cationic StyDex removal results were somewhat consistent using different wastewaters, with CV < 10% for most TrOC except MET (314%), OFL (223%), IPA (159%), CAF (165%), CBZ (44%) and TCPP (67%). The consistently high CV of MET, OFL, IPA, CAF, and TCPP experienced by the adsorbents indicate that their removal is more sensitive to variation in wastewater samples obtained at different times. Interestingly, we observed significantly enhanced MET removal from WW1 by all three adsorbents, compared to no removal in nanopure water or minimally enhanced removal in WW2 and WW3. We speculate the enhanced removal is related to MET participating in nonspecific interactions with wastewater constituents, which were subsequently removed by the adsorbents. Nonetheless, Cationic StyDex exhibited selective and effective TrOC removal similar to PSR2+ and experienced less removal inhibition compared to F600 in wastewater, indicating that Cationic StyDex is a promising adsorbent for wastewater remediation. This presents an opportunity in which Cationic StyDex may be used as a polishing step after GAC for hard-to-remove contaminants such as PFAS.

Adsorption Kinetics. Cationic StyDex demonstrated near-complete removal of six out of 13 TrOCs in both nanopure water and wastewater. We selected six TrOCs (PFOA, PFOS, PFHxA, PFHxS, BEZ, and DCF) to evaluate the adsorbents' adsorption kinetics over 24 h under similar experimental conditions. PFOS results are excluded from further analysis because its matrix-recovery concentrations in the absence of adsorbents were inconsistent in kinetics experiments. To enable quantitative comparisons among the adsorbents, we estimated pseudo-second-order adsorption rate constants (k_{obs}) from the adsorption kinetics data using eq 4. The resulting model fits are plotted in Figures S16−S18 and are summarized in Tables S7−S9. The R^2 of the model fits were generally >0.920 (Tables S7−S9). In nanopure water, Cationic StyDex achieved equilibrium and near-complete removal (>94%) for all five TrOCs within 5 min contact time (Figure 3A), as well as exhibited the highest k_{obs} from 35.6 to 120 g μg^{-1} h^{-1} for all five TrOCs out of the three adsorbents. These results are consistent with fast adsorption kinetics observed for cross-linked porous β-CD polymers in prior studies.[48] In contrast, F600 reached equilibrium within 30 min for PFHxS (k_{obs} = 19.1 g μg^{-1} h^{-1}), BEZ (k_{obs} = 21.8 g μg^{-1} h^{-1}), and DCF (k_{obs} = 20.9 g μg^{-1} h^{-1}), and within 1 h for PFOA (k_{obs} =

10.5 g μg^{-1} h^{-1}) and PFHxA (k_{obs} = 4.87 g μg^{-1} h^{-1}) (Figure 3C). Similarly, PSR2+ achieved equilibrium removal for most TrOCs within 30 min (k_{obs} = 11.6−73.9 g μg^{-1} h^{-1}) except within 2 h for BEZ (k_{obs} = 8.03 g μg^{-1} h^{-1}) (Figure 3E). It should be noted that both F600 and PSR2+ were ground and sieved into smaller particle sizes than their as-sold forms, which might result in faster kinetics than would be obtained from treatment systems that use these materials in their commercial form.

Two kinetics experiments were performed in wastewater (WW1 and WW2). The removal results at 24 h time points for each adsorbent are consistent with removal results from equilibrium adsorption experiments in WW1−WW3. F600 experienced the greatest inhibition in adsorption performance in wastewater, both in terms of kinetics and the extent of removal. For instance, the time for F600 to achieve equilibrium removal slowed from 1 to 8 h for all TrOCs in WW1, based on the plateauing of removal % curves between 8 and 24 h. The estimated k_{obs} of F600 for each TrOC also decreased significantly from 4.87 to 21.8 g μg^{-1} h^{-1} in nanopure water to 0.03−0.31 g μg^{-1} h^{-1} in WW1 (Tables S7 and S8). The time for PSR2+ to achieve equilibrium removal was somewhat slowed in WW1, from within 30 min for most TrOCs to within 2 h for PFOA (k_{obs} = 0.66 g μg^{-1} h^{-1}) and PFHxS (k_{obs} = 6.52 g μg^{-1} h^{-1}), and within 4 h for PFHxA (k_{obs} = 0.25 g μg^{-1} h^{-1}) and DCF (k_{obs} = 0.65 g μg^{-1} h^{-1}), whereas BEZ (k_{obs} = 0.62 g μg^{-1} h^{-1}) removal was further slowed from 2 to 8 h (Table S8). In contrast, the performance of Cationic StyDex was least inhibited by wastewater and reached equilibrium removal within 1 h for PFOA (k_{obs} = 6.42 g μg^{-1} h^{-1}), PFHxA (k_{obs} = 4.48 g μg^{-1} h^{-1}), PFHxS (k_{obs} = 11.0 g μg^{-1} h^{-1}), and DCF (k_{obs} = 3.57 g μg^{-1} h^{-1}), and within 2 h for BEZ (k_{obs} = 0.82 g μg^{-1} h^{-1}) in WW1, further highlighting the selectivity of Cationic StyDex toward target TrOCs within the complex wastewater matrix. In the case of F600, competitive adsorption and interaction with DOM are more likely to occur, resulting in slower and variable kinetics. We observed similar trends in the kinetics experiment performed in WW2 (Figure S19) as well as the corresponding estimated k_{obs} (Table S9). F600 experienced the greatest inhibition in adsorption kinetics and Cationic StyDex exhibited fastest kinetics. However, we also observed significant variation between results in WW1 and WW2, with earlier time points exhibiting largest CVs (>20%) for all three adsorbents (Tables S10−S12). F600 exhibited the most variable removal across the five TrOCs, which we attribute to its nonselective physisorption mechanism.

Adsorbent Affinity. We characterized the affinity of each adsorbent for the five TrOCs in wastewater using log-transformed distribution coefficients ($\log K_D$). Adsorption affinity is typically determined from adsorption isotherms fit to either the Langmuir or Freundlich equations. However, the five TrOCs are present at low concentrations (ng L^{-1}) in the wastewater, as evidenced by the background concentrations measured from multiple WW samples (Figure 1). Complete adsorption isotherms, which extend the testing concentration range above the environmentally relevant range of these TrOCs (e.g., ng L^{-1} to mg L^{-1}), were also generated for each adsorbent for the five TrOCs in wastewater. However, the $\log K_D$ values provide a better description of adsorbent affinity at low concentrations in natural water matrices, as we have previously demonstrated for studies in groundwater.[22,38] Log K_D values were calculated from the slope of the linear region of the adsorption isotherm (Figure S20). The R^2 values

of the linear regressions are generally >0.920, with the exceptions of Cationic StyDex/PFOA (0.911), PSR2+/PFHxS (0.831), Cationic StyDex/DCF (0.727), and F600/DCF (0.887). For comparison, we also analyzed the adsorption isotherm data with Langmuir and Freundlich models using eqs 6 and 7, respectively. The resulting model fits are plotted in Figure S20 and are summarized in Tables S13−S15, along with Log K_D values for comparison. It should be noted that isotherm data fit to the Freundlich model exhibited the lowest R^2 values.

According to unpaired t-tests, Cationic StyDex exhibited statistically significant ($p < 0.0001$) and higher log K_D values for the selected PFAS (1.82−3.58 L g^{-1}) than F600 (0.73−1.22 L g^{-1}), suggesting the presence of higher-affinity binding sites toward PFAS in Cationic StyDex than F600 in wastewater (Figure 4). Cationic StyDex also exhibited higher log K_D values
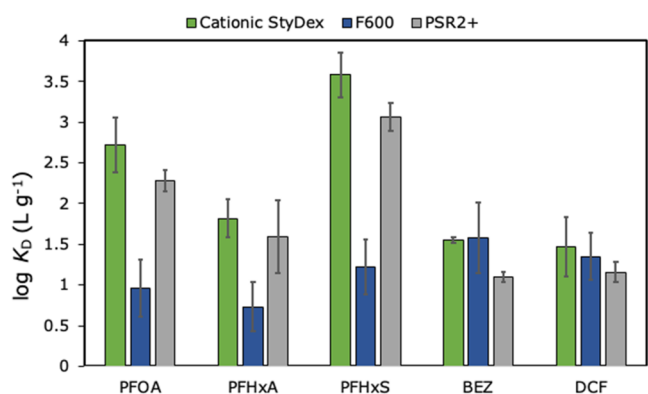

Figure 4. Average and standard deviation of the log-transformed distribution coefficients (log K_D) of Cationic StyDex (green bar), F600 (blue bar), and PSR2+ (gray bar) for each TrOC. Adsorbents were loaded at 100 mg L^{-1}. TrOCs were initially spiked between 100 and 8000 ng L^{-1}. The K_D values were calculated from the slope of the linear region of the adsorption isotherm for each adsorbent−TrOC pair.

for PFOA ($p < 0.0035$) and PFHxS ($p < 0.0026$) than PSR2+, while the two adsorbents did not exhibit differences in log K_D for PFHxA ($p = 0.295$) that were statistically significant. The same trend of adsorbent affinity is also observed based on

isotherm data fit to Langmuir and Freundlich models (Tables S13−S15). For example, Cationic StyDex exhibited higher K_L for PFAS (3.52−40.4 L μg^{-1}) compared to those of F600 (0.59−0.95 L μg^{-1}) and PSR2+ (3.35−10.3 L μg^{-1}). The high affinity of Cationic StyDex toward the selected PFAS in wastewater is consistent with equilibrium adsorption and kinetics results, in which Cationic StyDex demonstrated nearly complete PFAS removal with the fastest adsorption kinetics out of the three adsorbents. The affinity trend of Cationic StyDex toward the selected PFAS, PFHxS (3.58 ± 0.27 L g^{-1}) > PFOA (2.72 ± 0.33 L g^{-1}) > PFHxA (1.82 ± 0.24 L g^{-1}), is also consistent with our previous report that evaluated different sized β-CD polymer granules (prepared based on the previous generation of cross-linking chemistry) for PFAS removal in nanopure water.[49]

Cationic StyDex and F600 exhibited similar log K_D values for BEZ and DCF, which suggest that the binding sites present in each adsorbent have similar affinities for BEZ and DCF (Figure 4). However, F600 experienced more reduced BEZ and DCF removal and slower kinetics than Cationic StyDex in wastewater, which further highlight the selectivity of Cationic StyDex toward the target TrOCs in complex matrices. Overall, the adsorbent affinity experiment is consistent with previously measured isotherms for β-CD polymers, considering the significant and complex matrix effects associated with wastewater.

Regeneration Studies. The regeneration of spent Cationic StyDex was evaluated. Four regeneration and reuse cycles of 100 mg L^{-1} of Cationic StyDex were performed using either methanol or ethanol as the regenerating medium. Both methanol (Figure 5A) and ethanol (Figure S17) were found to be effective regenerating media following an overnight washing process based on the consistent TrOC removal efficiencies by Cationic StyDex over consecutive cycles. For example, PFOA and PFHxS removal from wastewater were near-complete over the four cycles, suggesting that Cationic StyDex can be regenerated without a significant decrease in removal performance. TrOCs were recovered by evaporating either methanol or ethanol on a standard rotary evaporator at 40 °C and reconstituting in water prior to quantification. Recoveries of PFOA, PFHxA, and PFHxS over four cycles were between 72 and 93% of the original spike concentration, whereas BEZ and
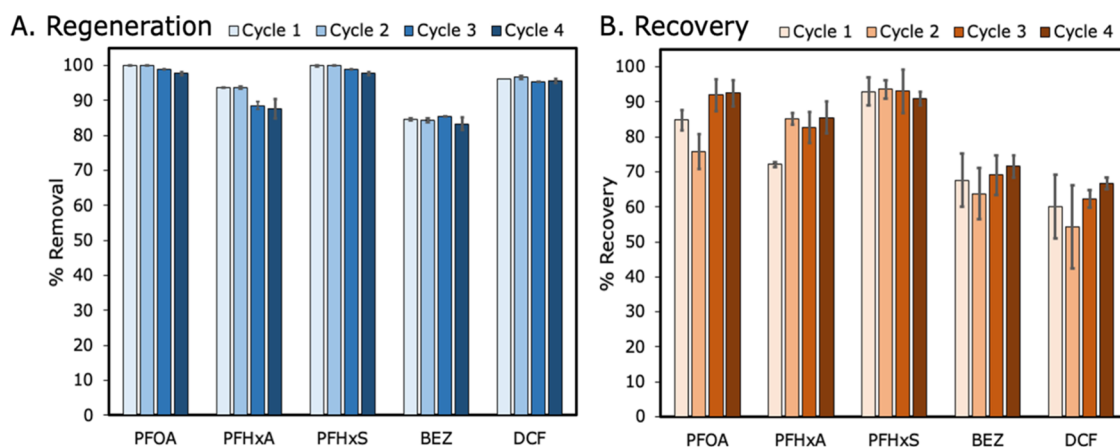

Figure 5. (A) Regeneration and reuse of Cationic StyDex in wastewater over four cycles using methanol. Adsorbent loading was originally 100 mg L^{-1} during the first removal cycle, but the loading decreased due to sample handling after each subsequent cycle. (B) Recovery of TrOCs from Cationic StyDex using methanol. An aliquot of TrOCs extracted in methanol was evaporated and reconstituted in equal volume of nanopure water for quantification. Error bars represent standard deviation of three replicates.
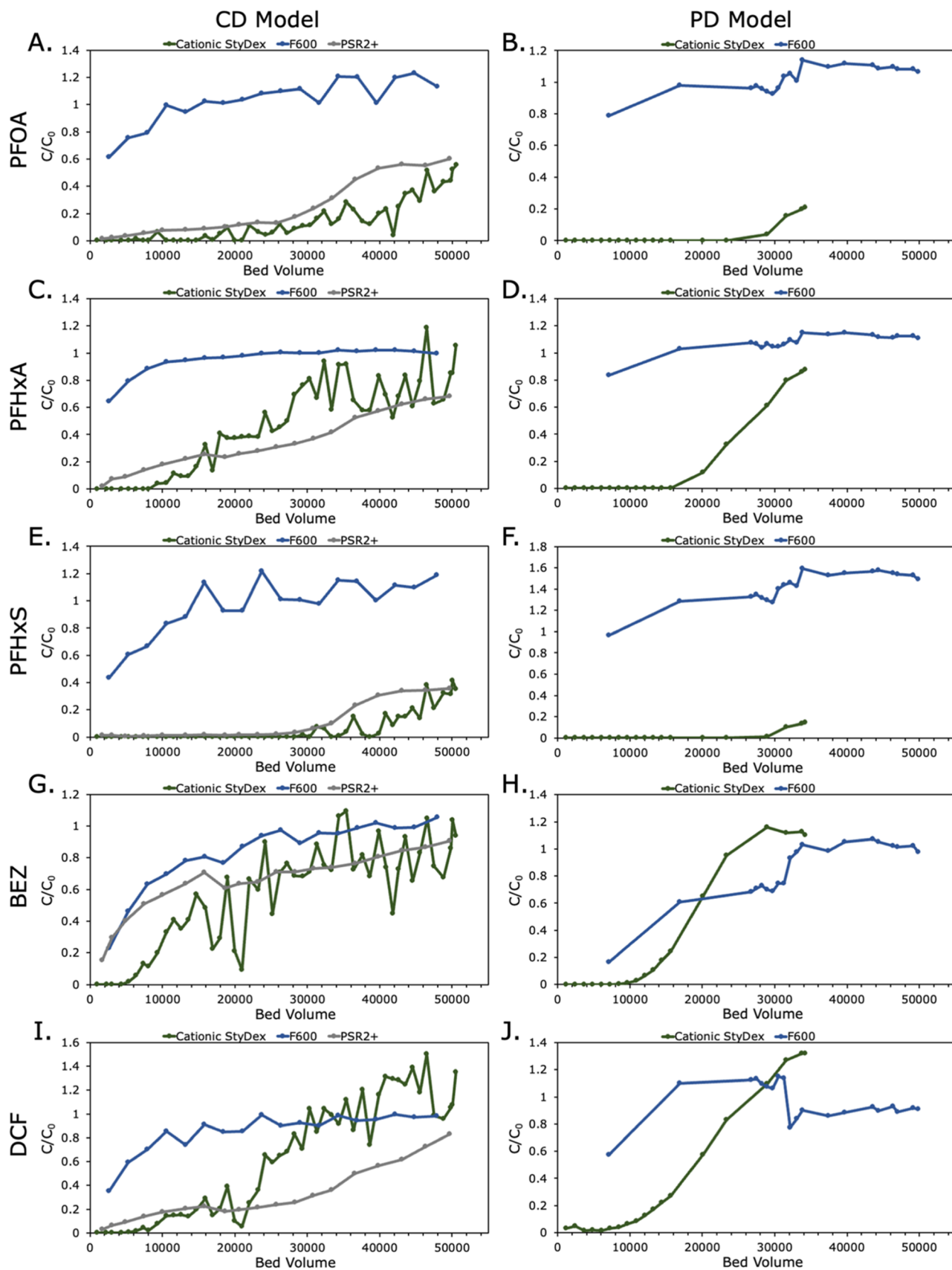
Figure 6. Breakthrough curves of the TrOCs under the assumption of constant diffusivity (left) and proportional diffusivity (right) using WW4–WW6. TrOCs were initially spiked at 500 ng L^{-1}.

DCF were recovered between 54 and 71% (Figure 5B). We attribute the lower recovery to potential losses in sample handling, considering that >90% removal by Cationic StyDex was achieved for PFAS and DCF, and >80% achieved for BEZ. Additionally, residual TrOCs may have remained within the adsorbent and subsequent removal performance was not affected due to initial TrOC concentration being significantly lower than the adsorbent capacity. Recovery of TrOCs from ethanol was generally lower than that from methanol (Figure S21B). We attribute the lower recovery to the solubility of the target TrOCs in ethanol. For instance, PFOA and PFOS have a higher solubility in methanol than in ethanol. Together, these results demonstrate the ease of regenerating spent Cationic StyDex through a simple solvent wash process, which is further supported by the recovery of TrOCs from the regenerating medium.

RSSCT Experiments. RSSCTs use fixed-bed mass transfer models to scale down column tests and simulate the full-scale performance of an adsorbent in a fraction of the time, resources, and cost of a pilot or full-scale study. Given that Cationic StyDex is a novel adsorbent, we evaluated its performance in wastewater by applying both the CD and PD models, based on eq 1. It should be noted that these models were developed for scaling activated carbon-based columns and may be specific to their distinct adsorption mechanisms and mass transfer limitations. Whether the scaling equation is applicable for the evaluation of IX resin or Cationic StyDex remains debatable. To support the RSSCT experimental design for ground PSR2+ in this study, we note that Schaefer et al. applied RSSCT under CD design ($X = 0$) to evaluate the scaling of ground and unground IX resins for the removal of PFAS. The authors demonstrated that RSSCT can be applied for the removal of the tested PFAS onto the IX resins.[50] We previously applied RSSCT under both CD and PD designs to evaluate different sized β-CD polymer (CDP) granules based on the previous generation of cross-linking chemistry and found that neither the assumption of CD nor PD was unequivocally appropriate for CDP granules.[49] Therefore, an improved understanding of mass transfer limitations of these novel adsorbents as a function of particle size will be desirable, as they are scaled to pilot-sized systems. Nevertheless, RSSCT experiments can be a valid approach to demonstrate the potential of implementing β-CD polymers under continuous flow systems.

For experiments using the CD design, BV10 and BV50 values, which are defined as the bed volume (BV) of each TrOC breakthrough to reach either 10 or 50% of the influent concentration, were estimated for each adsorbent for a comparative analysis. Based on BV10 values, Cationic StyDex outperformed F600 and PSR2+ for all five TrOCs (Figure 6, left). For example, BV10 of F600 for all five TrOCs occurred prior to 2600 BV, which was the first BV point collected. The BV10 values of PSR2+ for PFOA (16,000 BV), PFHxA (5000 BV), PFHxS (29,000 BV), BEZ (before 2600 BV), and DCF (6000 BV) were overall lower than those of Cationic StyDex for PFOA (21,000 BV), PFHxA (12,000 BV), PFHxS (33,000 BV), BEZ (6000 BV), and DCF (10,000 BV), in which a higher BV10 indicates later initial breakthrough times. However, the BV50 values suggest that the relative performance of PSR2+ and Cationic StyDex is more nuanced depending on the TrOC. For example, the BV50 values of PFHxA (25,000 BV for Cationic StyDex and 31,000 BV for PSR2+) and DCF (13,000 BV for Cationic StyDex and 36,000

BV for PSR2+) suggest that PSR2+ outperformed Cationic StyDex.

The early breakthrough times of all five TrOCs by F600 and of BEZ by PSR2+ may be explained by the fact that wastewaters (WW4–WW6) used in RSSCT experiments contained more COD and TDS than WW1–WW3 used in batch adsorption experiments (Table S2). Interestingly, the order of BV10 by Cationic StyDex for PFHxA (earliest) < PFOA < PFHxS (latest) corroborates with the literature observation,[41] such that perfluoroalkyl sulfonates can be removed more readily than carboxylates counterparts, which can be attributed to sulfonates having more fluorine (Figure 6B,F) for a given number of carbon. Additionally, longer-chain PFAS can be removed more readily than shorter-chain PFAS, based on PFOA and PFHxA results (Figure 6B,D).

For experiments applying the PD design (Figure 6, right), Cationic StyDex outperformed F600 for all five TrOCs, based on later breakthrough times. Generally speaking, the breakthrough curves of Cationic StyDex exhibited longer initial breakthrough times and steeper slopes than F600, which showed rapid initial breakthrough followed by a long flat slope. A steeper slope indicates that Cationic StyDex has a shorter mass transfer zone and faster kinetics than F600, which is supported by the adsorption kinetics results from batch adsorption experiments. The Cationic StyDex column clogged at 37,000 BV while F600 reached the full 50,000 BV, yielding incomplete breakthrough curves for PFOA, PFHxA, and PFHxS, but the observed breakthroughs are still sufficient to show improved performance of Cationic StyDex in terms of BV10. We attribute Cationic StyDex clogging to an insufficient rinse of the polymer after grinding, allowing dust particles to mix with the adsorbent.

RSSCTs conducted under the CD design showed, across all TrOCs, shorter breakthrough times compared to the RSSCTs conducted under the PD design. This is due to the shorter EBCTs in the CD RSSCTs, as the CD design yields a lower scaling factor. However, the relative performance and differences between Cationic StyDex and F600 remained consistent between the CD and PD designs. Bench-scale and pilot evaluations are needed to further evaluate the scalability of the Cationic StyDex performance in larger columns. Nevertheless, the RSSCT experiments demonstrate the practical application of Cationic StyDex for wastewater remediation. Future studies will focus on scaling StyDex polymerizations to enable large-scale evaluation and further tuning the polymer structure to improve TrOC removal.

ASSOCIATED CONTENT

Data Availability Statement
Data will be made available upon request.

Supporting Information
The Supporting Information is available free of charge at https://pubs.acs.org/doi/10.1021/acs.est.3c04233.

> TrOC and analytical methods, instrumentation parameters, wastewater characterization, RSSCT experimental design, monomer and polymer characterization, spike-recovery test for batch and RSSCT experiments, and additional batch adsorption experiments, such as equilibrium removal experiments in WW2 and WW3, adsorption kinetics experiment in WW2, pseudo-second-order, Langmuir, and Freundlich model fits, and regeneration study in ethanol (PDF)

■ AUTHOR INFORMATION

Corresponding Author

William R. Dichtel − *Department of Chemistry, Northwestern University, Evanston, Illinois 60208, United States;* orcid.org/0000-0002-3635-6119; Phone: (847)-467-6031; Email: wdichtel@northwestern.edu

Authors

Zhi-Wei Lin − *Department of Chemistry, Northwestern University, Evanston, Illinois 60208, United States;* orcid.org/0000-0002-6465-3698

Emma F. Shapiro − *Department of Civil and Environmental Engineering, Northwestern University, Evanston, Illinois 60208, United States*

Francisco J. Barajas-Rodriguez − *AECOM, Dallas, Texas 75240, United States;* orcid.org/0000-0003-0325-6709

Arsen Gaisin − *Department of Chemistry, Northwestern University, Evanston, Illinois 60208, United States*

Mohamed Ateia − *Department of Chemical and Biomolecular Engineering, Rice University, Houston, Texas 77005, United States;* orcid.org/0000-0002-3524-5513

John Currie − *AECOM, Dallas, Texas 75240, United States*

Damian E. Helbling − *School of Civil and Environmental Engineering, Cornell University, Ithaca, New York 14853, United States;* orcid.org/0000-0003-2588-145X

Rosa Gwinn − *AECOM, Dallas, Texas 75240, United States*

Aaron I. Packman − *Department of Civil and Environmental Engineering, Northwestern University, Evanston, Illinois 60208, United States*

Complete contact information is available at:
https://pubs.acs.org/10.1021/acs.est.3c04233

Notes

The authors declare the following competing financial interest(s): Northwestern University has filed one or more patent applications related to the findings of this manuscript. W.R.D. owns equity and/or stock options in Cyclopure, Inc. (Cyclopure), which is commercializing β-CD polymers. Cyclopure did not contribute to this research.

■ REFERENCES

(1) Capodaglio, A. G. Fit-for-purpose urban wastewater reuse: Analysis of issues and available technologies for sustainable multiple barrier approaches. *Crit. Rev. Environ. Sci. Technol.* **2021**, *51* (15), 1619−1666.

(2) Khan, S. A. R.; Ponce, P.; Yu, Z.; Golpira, H.; Mathew, M. Environmental technology and wastewater treatment: Strategies to achieve environmental sustainability. *Chemosphere* **2022**, *286*, No. 131532.

(3) Ofori, S.; Puskacova, A.; Ruzickova, I.; Wanner, J. Treated wastewater reuse for irrigation: Pros and cons. *Sci. Total Environ.* **2021**, *760*, No. 144026.

(4) Saliu, T. D.; Oladoja, N. A. Nutrient recovery from wastewater and reuse in agriculture: a review. *Environ. Chem. Lett.* **2021**, *19* (3), 2299−2316.

(5) Almeida, J.; Monahan, A.; Dionisio, J.; Delgado, F.; Magro, C. Sustainability assessment of wastewater reuse in a Portuguese military airbase. *Sci. Total Environ.* **2022**, *851*, No. 158329.

(6) Liao, Z.; Chen, Z.; Xu, A.; Gao, Q.; Song, K.; Liu, J.; Hu, H. Y. Wastewater treatment and reuse situations and influential factors in major Asian countries. *J. Environ. Manage.* **2021**, *282*, No. 111976.

(7) Tampo, L.; Alfa-Sika Mande, S. L.; Adekanmbi, A. O.; Boguido, G.; Akpataku, K. V.; Ayah, M.; Tchakala, I.; Gnazou, M. D. T.; Bawa, L. M.; Djaneye-Boundjou, G.; Alhassan, E. H. Treated wastewater suitability for reuse in comparison to groundwater and surface water in a peri-urban area: Implications for water quality management. *Sci. Total Environ.* **2022**, *815*, No. 152780.

(8) UN-Water. *The United Nations World Water Development Report 2021*; United Nations Educational, Scientific and Cultural Organization, 2021.

(9) Lyu, S.; Wu, L.; Wen, X.; Wang, J.; Chen, W. Effects of reclaimed wastewater irrigation on soil-crop systems in China: A review. *Sci. Total Environ.* **2022**, *813*, No. 152531.

(10) Poustie, A.; Yang, Y.; Verburg, P.; Pagilla, K.; Hanigan, D. Reclaimed wastewater as a viable water source for agricultural irrigation: A review of food crop growth inhibition and promotion in the context of environmental change. *Sci. Total Environ.* **2020**, *739*, No. 139756.

(11) Richardson, S. D.; Kimura, S. Y. Emerging environmental contaminants: Challenges facing our next generation and potential engineering solutions. *Environ. Technol. Innov.* **2017**, *8*, 40−56.

(12) Spahr, S.; Teixidó, M.; Sedlak, D. L.; Luthy, R. G. Hydrophilic trace organic contaminants in urban stormwater: occurrence, toxicological relevance, and the need to enhance green stormwater infrastructure. *Environ. Sci.: Water Res. Technol.* **2020**, *6* (1), 15−44.

(13) Schulze, S.; Zahn, D.; Montes, R.; Rodil, R.; Quintana, J. B.; Knepper, T. P.; Reemtsma, T.; Berger, U. Occurrence of emerging persistent and mobile organic contaminants in European water samples. *Water Res.* **2019**, *153*, 80−90.

(14) Nzeribe, B. N.; Crimi, M.; Mededovic Thagard, S.; Holsen, T. M. Physico-Chemical Processes for the Treatment of Per- And Polyfluoroalkyl Substances (PFAS): A review. *Crit. Rev. Environ. Sci. Technol.* **2019**, *49* (10), 866−915.

(15) Li, F.; Duan, J.; Tian, S.; Ji, H.; Zhu, Y.; Wei, Z.; Zhao, D. Short-chain per- and polyfluoroalkyl substances in aquatic systems: Occurrence, impacts and treatment. *Chem. Eng. J.* **2020**, *380*, No. 122506. DOI: 10.1016/j.cej.2019.122506.

(16) Nøst, T. H.; Vestergren, R.; Berg, V.; Nieboer, E.; Odland, J. O.; Sandanger, T. M. Repeated measurements of per- and polyfluoroalkyl substances (PFASs) from 1979 to 2007 in males from Northern Norway: assessing time trends, compound correlations and relations to age/birth cohort. *Environ. Int.* **2014**, *67*, 43−53.

(17) Margenat, A.; Matamoros, V.; Diez, S.; Canameras, N.; Comas, J.; Bayona, J. M. Occurrence and human health implications of chemical contaminants in vegetables grown in peri-urban agriculture. *Environ. Int.* **2019**, *124*, 49−57.

(18) Phoon, B. L.; Ong, C. C.; Mohamed Saheed, M. S.; Show, P. L.; Chang, J. S.; Ling, T. C.; Lam, S. S.; Juan, J. C. Conventional and emerging technologies for removal of antibiotics from wastewater. *J. Hazard. Mater.* **2020**, *400*, No. 122961.

(19) Rout, P. R.; Zhang, T. C.; Bhunia, P.; Surampalli, R. Y. Treatment technologies for emerging contaminants in wastewater treatment plants: A review. *Sci. Total Environ.* **2021**, *753*, No. 141990.

(20) Sá, M. F.; Castro, V.; Gomes, A. I.; Morais, D. F. S.; Silva Braga, R.; Saraiva, I.; Souza-Chaves, B. M.; Park, M.; Fernandez-Fernandez, V.; Rodil, R.; Montes, R.; Quintana, J. B.; Vilar, V. J. P. Tracking pollutants in a municipal sewage network impairing the operation of a wastewater treatment plant. *Sci. Total Environ.* **2022**, *817*, No. 152518.

(21) Varsha, M.; Senthil Kumar, P.; Senthil Rathi, B. A review on recent trends in the removal of emerging contaminants from aquatic

environment using low-cost adsorbents. *Chemosphere* **2022**, *287* (3), No. 132270.

(22) Ching, C.; Klemes, M. J.; Trang, B.; Dichtel, W. R.; Helbling, D. E. beta-Cyclodextrin polymers with different cross-linkers and ion-exchange resins exhibit variable adsorption of anionic, zwitterionic, and nonionic PFASs. *Environ. Sci. Technol.* **2020**, *54* (19), 12693−12702.

(23) Wang, R.; Lin, Z. W.; Klemes, M. J.; Ateia, M.; Trang, B.; Wang, J.; Ching, C.; Helbling, D. E.; Dichtel, W. R. A Tunable Porous beta-Cyclodextrin Polymer Platform to Understand and Improve Anionic PFAS Removal. *ACS Cent. Sci.* **2022**, *8* (5), 663−669.

(24) Huang, Q.; Chai, K.; Zhou, L.; Ji, H. A phenyl-rich β-cyclodextrin porous crosslinked polymer for efficient removal of aromatic pollutants: Insight into adsorption performance and mechanism. *Chem. Eng. J.* **2020**, *387*, No. 124020, DOI: 10.1016/j.cej.2020.124020.

(25) Qin, X.; Bai, L.; Tan, Y.; Li, L.; Song, F.; Wang, Y. β-Cyclodextrin-crosslinked polymeric adsorbent for simultaneous removal and stepwise recovery of organic dyes and heavy metal ions: Fabrication, performance and mechanisms. *Chem. Eng. J.* **2019**, *372*, 1007−1018.

(26) Alsbaiee, A.; Smith, B. J.; Xiao, L.; Ling, Y.; Helbling, D. E.; Dichtel, W. R. Rapid removal of organic micropollutants from water by a porous beta-cyclodextrin polymer. *Nature* **2016**, *529* (7585), 190−194.

(27) Guo, R.; Liu, H.; Yang, K.; Wang, S.; Sun, P.; Gao, H.; Wang, B.; Chen, F. beta-Cyclodextrin Polymerized in Cross-Flowing Channels of Biomass Sawdust for Rapid and Highly Efficient Pharmaceutical Pollutants Removal from Water. *ACS Appl. Mater. Interfaces* **2020**, *12* (29), 32817−32826.

(28) Tian, B.; Hua, S.; Tian, Y.; Liu, J. Cyclodextrin-based adsorbents for the removal of pollutants from wastewater: a review. *Environ. Sci. Pollut. Res.* **2021**, *28* (2), 1317−1340.

(29) Ling, Y.; Klemes, M. J.; Xiao, L.; Alsbaiee, A.; Dichtel, W. R.; Helbling, D. E. Benchmarking Micropollutant Removal by Activated Carbon and Porous beta-Cyclodextrin Polymers under Environmentally Relevant Scenarios. *Environ. Sci. Technol.* **2017**, *51* (13), 7590−7598.

(30) Crini, G. Review: a history of cyclodextrins. *Chem. Rev.* **2014**, *114* (21), 10940−10975.

(31) Weiss-Errico, M. J.; O'Shea, K. E. Detailed NMR investigation of cyclodextrin-perfluorinated surfactant interactions in aqueous media. *J. Hazard Mater.* **2017**, *329*, 57−65.

(32) Klemes, M. J.; Ling, Y.; Ching, C.; Wu, C.; Xiao, L.; Helbling, D. E.; Dichtel, W. R. Reduction of a Tetrafluoroterephthalonitrile-beta-Cyclodextrin Polymer to Remove Anionic Micropollutants and Perfluorinated Alkyl Substances from Water. *Angew. Chem., Int. Ed.* **2019**, *58* (35), 12049−12053.

(33) Li, C.; Klemes, M. J.; Dichtel, W. R.; Helbling, D. E. Tetrafluoroterephthalonitrile-crosslinked beta-cyclodextrin polymers for efficient extraction and recovery of organic micropollutants from water. *J. Chromatogr. A* **2018**, *1541*, 52−56.

(34) Xiao, L.; Ching, C.; Ling, Y.; Nasiri, M.; Klemes, M. J.; Reineke, T. M.; Helbling, D. E.; Dichtel, W. R. Cross-linker Chemistry Determines the Uptake Potential of Perfluorinated Alkyl Substances by β-Cyclodextrin Polymers. *Macromolecules* **2019**, *52* (10), 3747−3752.

(35) Xiao, L.; Ling, Y.; Alsbaiee, A.; Li, C.; Helbling, D. E.; Dichtel, W. R. beta-Cyclodextrin Polymer Network Sequesters Perfluorooctanoic Acid at Environmentally Relevant Concentrations. *J. Am. Chem. Soc.* **2017**, *139* (23), 7689−7692.

(36) Wu, C.; Klemes, M. J.; Trang, B.; Dichtel, W. R.; Helbling, D. E. Exploring the factors that influence the adsorption of anionic PFAS on conventional and emerging adsorbents in aquatic matrices. *Water Res.* **2020**, *182*, No. 115950.

(37) Ling, Y.; Alzate-Sanchez, D. M.; Klemes, M. J.; Dichtel, W. R.; Helbling, D. E. Evaluating the effects of water matrix constituents on micropollutant removal by activated carbon and beta-cyclodextrin polymer adsorbents. *Water Res.* **2020**, *173*, No. 115551.

(38) Ling, Y.; Klemes, M. J.; Steinschneider, S.; Dichtel, W. R.; Helbling, D. E. QSARs to predict adsorption affinity of organic micropollutants for activated carbon and beta-cyclodextrin polymer adsorbents. *Water Res.* **2019**, *154*, 217−226.

(39) Ateia, M.; Helbling, D. E.; Dichtel, W. R. Best practices for evaluating new materials as adsorbents for water treatment. *ACS Mater. Lett.* **2020**, *2* (11), 1532−1544.

(40) Tang, Y.; Lee, C.-S.; Walker, H.; Gobler, C.; Apul, O.; Venkatesan, A. K.; Mao, X. Effect of residual H2O2 on the removal of advanced oxidation byproducts by two types of granular activated carbon. *J. Environ. Chem. Eng.* **2021**, *9* (6), No. 106838, DOI: 10.1016/j.jece.2021.106838.

(41) Ellis, A. C.; Liu, C. J.; Fang, Y.; Boyer, T. H.; Schaefer, C. E.; Higgins, C. P.; Strathmann, T. J. Pilot study comparison of regenerable and emerging single-use anion exchange resins for treatment of groundwater contaminated by per- and polyfluoroalkyl substances (PFASs). *Water Res.* **2022**, *223*, No. 119019.

(42) Crittenden, J. C.; Reddy, P. S.; Arora, H.; Trynoski, J.; Hand, D. W.; Perram, D. L.; Summers, R. S. Predicting GAC performance with rapid small-scale column tests. *J. Am. Water Work Assoc.* **1991**, *83* (1), 77−87.

(43) Ho, Y. S.; McKay, G. Pseudo-second order model for sorption processes. *Process Biochem.* **1999**, *34*, 451−456.

(44) Schaefer, C. E.; Hooper, J. L.; Strom, L. E.; Abusallout, I.; Dickenson, E. R. V.; Thompson, K. A.; Mohan, G. R.; Drennan, D.; Wu, K.; Guelfo, J. L. Occurrence of quantifiable and semi-quantifiable poly- and perfluoroalkyl substances in united states wastewater treatment plants. *Water Res.* **2023**, *233*, No. 119724.

(45) Thompson, K. A.; Mortazavian, S.; Gonzalez, D. J.; Bott, C.; Hooper, J.; Schaefer, C. E.; Dickenson, E. R. V. Poly- and Perfluoroalkyl Substances in Municipal Wastewater Treatment Plants in the United States: Seasonal Patterns and Meta-Analysis of Long-Term Trends and Average Concentrations. *ACS ES&T Water* **2022**, *2* (5), 690−700.

(46) Khasawneh, O. F. S.; Palaniandy, P. Occurrence and removal of pharmaceuticals in wastewater treatment plants. *Process Saf. Environ. Prot.* **2021**, *150*, 532−556.

(47) Pasquini, L.; Munoz, J. F.; Pons, M. N.; Yvon, J.; Dauchy, X.; France, X.; Le, N. D.; France-Lanord, J.; Gorner, T. Occurrence of eight household micropollutants in urban wastewater and their fate in a wastewater treatment plant. Statistical evaluation. *Sci. Total Environ.* **2014**, *481*, 459−468.

(48) Klemes, M. J.; Skala, L. P.; Ateia, M.; Trang, B.; Helbling, D. E.; Dichtel, W. R. Polymerized Molecular Receptors as Adsorbents to Remove Micropollutants from Water. *Acc. Chem. Res.* **2020**, *53* (10), 2314−2324.

(49) Ching, C.; Lin, Z.-W.; Dichtel, W. R.; Helbling, D. E. Evaluating the Performance of Novel Cyclodextrin Polymer Granules to Remove Perfluoroalkyl Acids (PFAAs) from Water. *ACS ES&T Eng.* **2023**, *3*, 661−670, DOI: 10.1021/acsestengg.2c00379.

(50) Schaefer, C. E.; Nguyen, D.; Ho, P.; Im, J.; LeBlanc, A. Assessing Rapid Small-Scale Column Tests for Treatment of Perfluoroalkyl Acids by Anion Exchange Resin. *Ind. Eng. Chem. Res.* **2019**, *58* (22), 9701−9706.